

# Fire Resistance of Exterior Walls: Model and Full-scale Test

H. TAKEDA  
Fire Research Canada (LGS)  
6148 Voyageur Dr.  
Orleans, Ontario, K1C 2W3, Canada

## ABSTRACT

The paper describes a heat transfer model for prediction of the thermal response of wood-framed exterior walls constructed with 105 mm by 105 mm wood post, gypsum board attached to the wood post on the interior side of the wall, insulation foam between posts, an air cavity of ventilation purposes, and a 12 mm thick non-combustible (ceramic) exterior siding attached to the wall over the wood strapping. This is a typical Japanese 'post and beam' type exterior walls. This paper examines the fire resistance of this type of wall when the exterior face of the wall is exposed to fire. The model calculates heat transfer through the siding, the air cavity, wood strapping, foamed-plastic insulation, wood posts and the gypsum board on the interior face. Mass transfer was not considered in this model. When the calculated results were compared to the results from full-scale fire-endurance tests, very good agreement was observed. The paper also describes the effect of the thickness and density of the exterior siding and gypsum board on the fire resistance of the exterior walls.

**KEYWORDS:** heat transfer, modeling, fire resistance, exterior siding, wood-framed walls, foamed plastic insulation, gypsum board, full-scale fire tests

## INTRODUCTION

Wood-framed exterior walls with an air cavity directly behind the exterior siding are increasing in popularity in recent years in Japan because air circulation through that external air cavity assists in preventing condensation of moisture within the walls. Figure 1 illustrates a typical 'post and beam' type wood-framed exterior wall with such

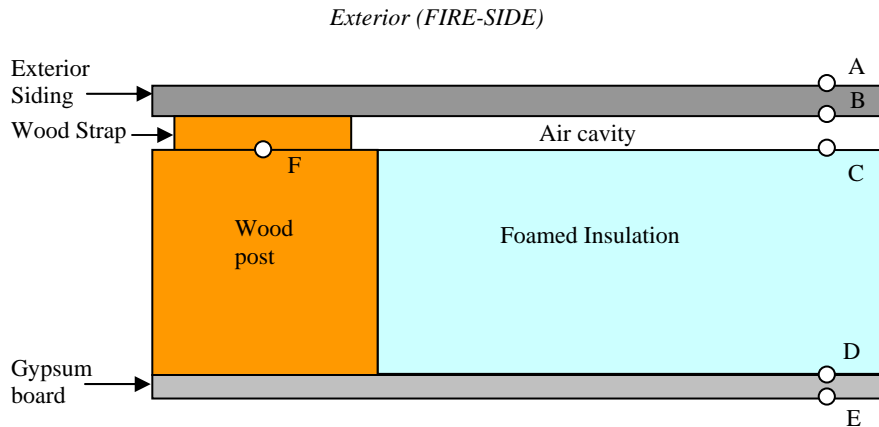


Fig. 1. Structure of the exterior wall (A to F indicate thermocouple locations).

an external air cavity. It might reasonably be expected that this siding cavity would not only prevent moisture condensation in the wall but would also improve the fire resistance of the assembly. The present paper describes a computer model to predict the thermal response of such wood-framed exterior wall assemblies when the exterior siding is exposed to fire. Calculated results from the model compare to the results from two full-scale fire endurance tests for the model validation. The paper also discusses the effect of the thickness and density of exterior siding and gypsum board on the fire resistance of this type of exterior walls.

## MODEL THEORY AND EQUATIONS

Heat transfer through the solid components satisfies the two-dimensional heat conduction equation.

$$C_p \rho (\partial T / \partial t) = \partial / \partial x (k \partial T / \partial x) + \partial / \partial y (k \partial T / \partial y) \quad (1)$$

Where  $C_p$  is a specific heat (J/kg•K),  $\rho$  is density (kg/m<sup>3</sup>) and  $k$  is a thermal conductivity (W/m•K),  $T$  is temperature (K),  $t$  is time (s), and  $x$  and  $y$  are space coordinates (m). The above thermo-physical properties  $C_p$ ,  $\rho$  and  $k$  are defined as functions of temperatures [1-7]. Boundary conditions at the exposed surface of the exterior siding are given by balancing heat conduction at the surface with the radiative and convective heat input [2]:

$$-k_s (\partial T / \partial x) = h_f (T_f - T_{sf}) + \epsilon_{ff} \sigma (T_f^4 - T_{sf}^4) \quad (2)$$

where  $T_{sf}$  is the surface temperature of the exterior siding,  $T_f$  is the furnace gas temperature,  $h_f$  is the convective heat transfer coefficient (W/m<sup>2</sup>•K) between the surface of the exterior siding and the furnace gas,  $\sigma$  is the Stephan-Boltzmann constant for radiation and  $\epsilon_{ff}$  is the effective emissivity calculated from the furnace gas emissivity  $\epsilon_f$  and surface emissivity of the exterior siding  $\epsilon_s$  [1].

$$\epsilon_{ff} = 1 / (1 / \epsilon_f + 1 / \epsilon_s - 1) \quad (3)$$

The boundary condition at the surface of the exterior siding on the cavity-side can be described as:

$$-k_s (\partial T / \partial x) = h_a (T_{sc} - T_c) + \epsilon \sigma F_{C12} (T_{sc}^4 - T_{ic}^4) + \epsilon \sigma F_{C13} (T_{sc}^4 - T_{is}^4) \quad (4)$$

where  $T_{sc}$  is the surface temperature of the exterior siding on the cavity-side,  $T_c$  is the cavity gas temperature,  $T_{is}$  is the surface temperature of sides of the wood strap facing the cavity and  $h_a$  is the convective heat transfer coefficient (W/m<sup>2</sup>•K) between the surface of the exterior siding and the cavity gas.

The boundary condition at the surface of the foamed insulation which faces the cavity gas can be described as:

$$-k_i (\partial T / \partial x) = h_a (T_c - T_{ic}) + \epsilon \sigma F_{C12} (T_{sc}^4 - T_{ic}^4) + \epsilon \sigma F_{C23} (T_{is}^4 - T_{ic}^4) \quad (5)$$

where  $T_{ic}$  is the surface temperature of the foamed insulation facing the cavity gas and  $k_i$  is the thermal conductivity of insulation.  $F_{C12}$ ,  $F_{C13}$  and  $F_{C23}$  are the view factors for

radiative heat exchange [1,2]. As the insulation shrinks at elevated temperatures [2,4], the depth of the siding cavity increases with time (see Fig. 2). Since the view factors were defined as functions of the depth and width of the cavity [1-3], those factors,  $F_{C12}$ ,  $F_{C13}$  and  $F_{C23}$  are changing with time. In addition, the surface of the sides of post is exposed to

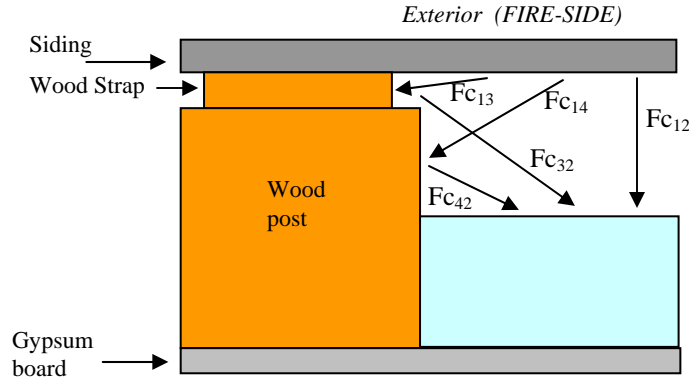


Fig. 2. View factors in the cavity when insulation shrinks.

the siding cavity (Fig. 2). Thereby, new view factors  $F_{C14}$  and  $F_{C42}$  should be considered. Accordingly, the boundary conditions Eqs. 4 and 5 should be changed to the following Eqs. 6 and 7, when foamed insulation shrinks.

$$-k_s (\partial T / \partial x) = h_a (T_{sc} - T_c) + \epsilon \sigma F_{C12} (T_{sc}^4 - T_{ic}^4) + \epsilon \sigma F_{C13} (T_{sc}^4 - T_{is}^4) + \epsilon \sigma F_{C14} (T_{sc}^4 - T_{wc}^4) \quad (6)$$

$$-k_i (\partial T / \partial x) = h_a (T_c - T_{ic}) + \epsilon \sigma F_{C12} (T_{sc}^4 - T_{ic}^4) + \epsilon \sigma F_{C32} (T_{is}^4 - T_{ic}^4) + \epsilon \sigma F_{C42} (T_{wc}^4 - T_{ic}^4) \quad (7)$$

And the boundary condition at the surface of the wood post exposed to the siding cavity can be described as:

$$-k_w (\partial T / \partial y) = h_a (T_{wc} - T_c) + \epsilon \sigma F_{C14} (T_{sc}^4 - T_{wc}^4) + \epsilon \sigma F_{C42} (T_{wc}^4 - T_{ic}^4) \quad (8)$$

Where  $T_{wc}$  is the surface temperature of the sides of wood post.

At the interfaces between the siding and wood strap, and the wood strap and wood post, the following continuity equations were assumed,

$$k_s (\partial T / \partial x)_{siding} = k_w (\partial T / \partial x)_{strap} \quad (9)$$

$$k_w (\partial T / \partial x)_{strap} = k_w (\partial T / \partial x)_{post} \quad (10)$$

Where  $k_s$  and  $k_w$  are the thermal conductivities of exterior siding and wood respectively. Also similar continuity equations were assumed at the interface between foamed insulation and the side surface of the post,

$$k_w (\partial T/\partial y)_{\text{post}} = k_i (\partial T/\partial y)_{\text{insulation}} \quad (11)$$

and at the interface between foamed insulation and gypsum board.

$$k_i (\partial T/\partial x)_{\text{insulation}} = k_g (\partial T/\partial x)_{\text{gypsum}} \quad (12)$$

Where  $k_g$  is the thermal conductivity of gypsum board.

The boundary condition at the surface of gypsum board on the ambient side (inside the building) can be described as:

$$-k_g (\partial T/\partial x) = h_c(T_{\text{ga}} - T_a) + \sigma(T_a^4 - T_{\text{ga}}^4) \quad (13)$$

Where  $T_a$  is the ambient gas temperature.

The above equations Eqs. 1 to 13 were solved using the finite difference method. The grid size for the x-direction,  $\Delta x$ , was defined as 0.0015m and for y-direction,  $\Delta y = 0.003\text{m}$ , and the time step 1 sec. Thermal properties in those equations, specific heat  $C_p$ , thermal conductivity  $k$  and density  $\rho$  were defined as functions of temperatures [1-3]. Heat transfer coefficient  $h_f$  and  $h_a$  were assumed to be 25 and 9  $\text{W/m}^2\cdot\text{K}$  respectively. The emissivity within the assembly  $\epsilon$  was assumed to be unity. The computer program was written in C++ and the user interface and graphics display were created in Microsoft Visual C++ and MFC.

## THERMAL PROPERTIES

Thermal conductivities of exterior siding [6], wood [1], foamed insulation EPS (extended polystyrene foam) [2,4] and gypsum board [1] used in this model are shown in Fig. 3 as a function of temperature.

Specific heat of exterior siding [6], wood [1], foamed insulation EPS [6] and gypsum board [1] used in this model are shown in Fig. 4 as a function of temperature.

Specific heat of gypsum board has a sharp peak at around 102°C and second small peak at 660°C [1]. Specific heat of wood also has a peak at around 120°C and second peak at 220°C [1]. On the other hand, those of EPS and exterior siding are relative flat within the temperature range between 0°C and 1000°C, which are between 1.2 to 1.4 (kJ/kg) [6].

## FULL-SCALE FIRE TEST

Two full-scale fire endurance tests were conducted for the model validation by the Japan Testing Center for Construction Materials (JTCCM). Figure 5 shows the JTCCM test apparatus (furnace) and exterior wall specimen [2]. Test specimens were constructed with 12 mm thick ceramic exterior siding, 18 mm by 90 mm wood strapping, 105 mm thick expanded polystyrene foam (EPS), 105 mm by 105 mm wood post and 9.5 mm thick gypsum board. The density of the ceramic siding used in these tests was 1,250  $\text{kg/m}^3$  and the moisture content was 3.1%. The density of EPS was 33  $\text{kg/m}^3$ . Regular Japanese gypsum board (660  $\text{kg/m}^3$ ) was used as the interior wall lining.

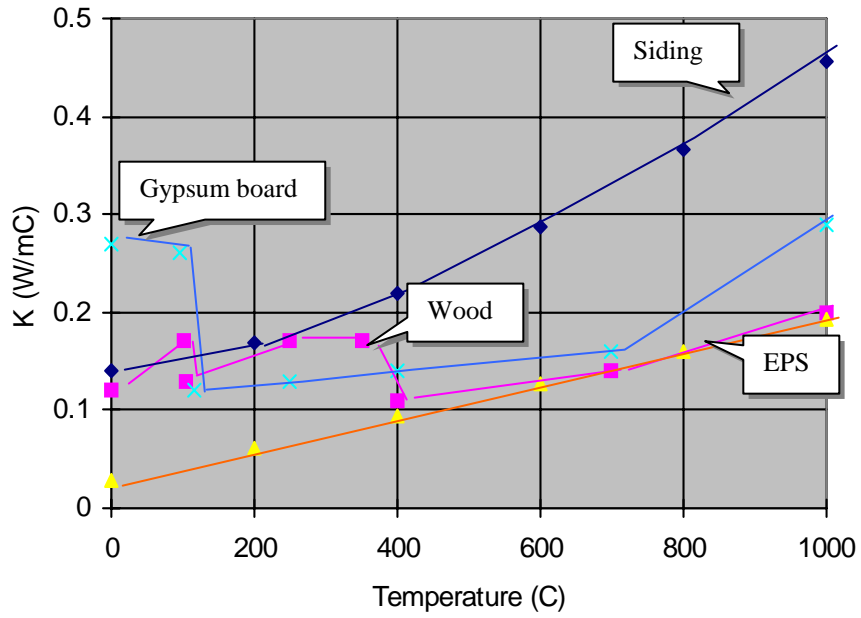


Fig. 3. Thermal conductivities of exterior siding, wood, EPS (extended polystyrene foam) and gypsum board as a function of temperature.

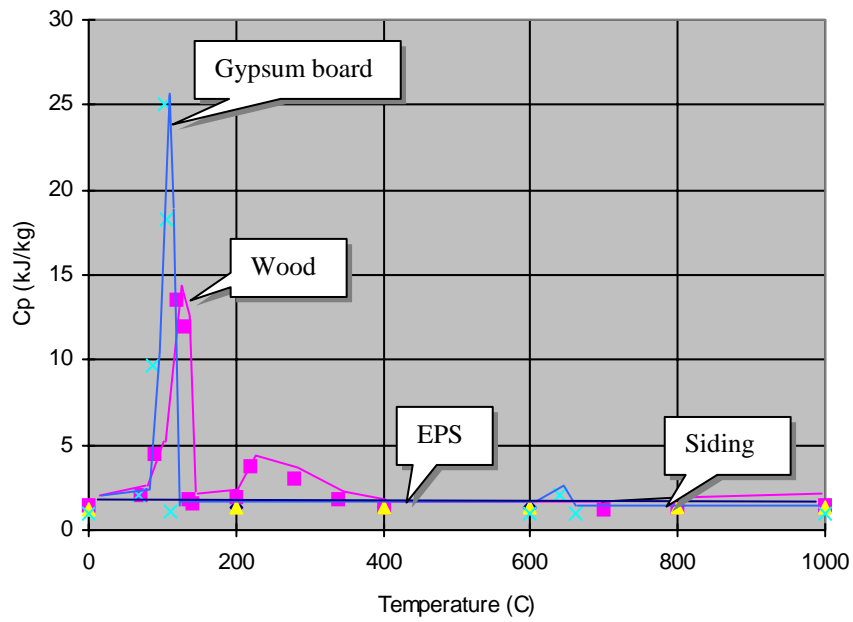


Fig. 4. Specific heat of exterior siding, wood, EPS (polystyrene foam) and gypsum board as a function of temperature.

The test specimen was installed in the furnace with the exterior siding facing the gas burners. The furnace was fueled by premixed propane-air burners. The heating curve used in the test was that described in ISO834 [8]. Thermocouples were installed on the surfaces of the various components in order to measure the temperatures of the surface of the exterior siding facing the cavity, B, the surface of the foamed insulation facing the cavity, C, the interface between insulation and gypsum board, D, ambient side of the assembly, E, and the interface between the wood strap and post F (see Fig. 1).

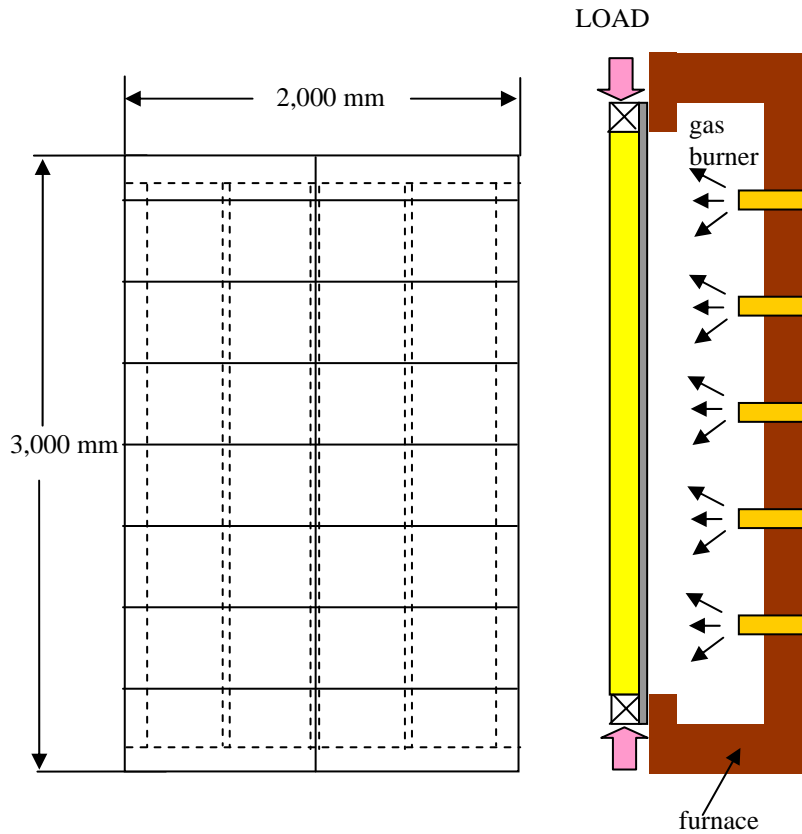


Fig. 5. Test apparatus and exterior wall test specimen.

### COMPARISON BETWEEN TEST RESULTS AND MODEL PREDICTIONS

Figure 6 shows the time/temperature curves obtained from the full-scale test (dashed lines) at locations B to F (those locations are indicated in Fig. 1). Theoretical predictions from the model are shown in the same figure as solid lines. Comparing the model predictions to the test results, a very good agreement was observed. The model also predicts char formation in wood strapping and post, and the melting behavior of the foamed insulation, EPS. The time when the EPS began to melt was predicted to be 8 min 26 sec, and the model predicted that all the EPS would be melted away at 21 min 51 sec. The time until charring of the wood strapping would commence was predicted to be 14 min 56 sec, and the time when it was predicted that all the wood strapping would be converted to char was 46 min 30 sec.

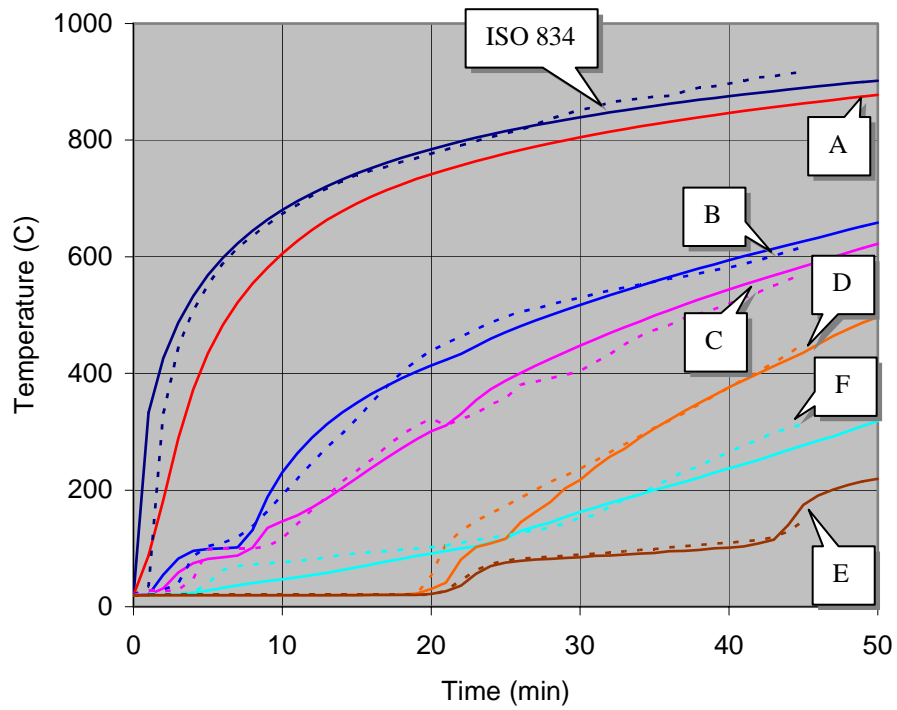


Fig. 6. Test results (dashed lines) and model prediction (solid lines).

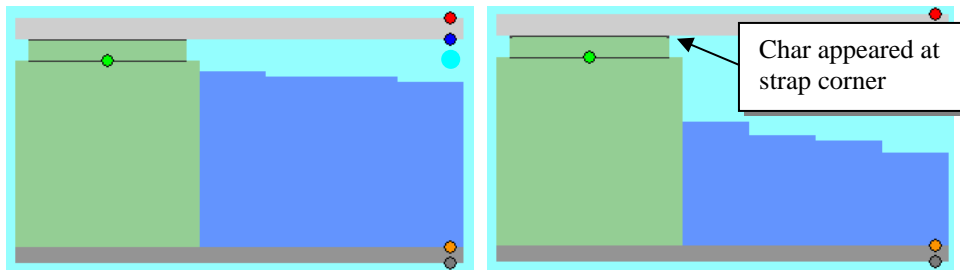


Fig. 7. Melting behavior of foamed insulation at 10min (left) and 15 min (right).

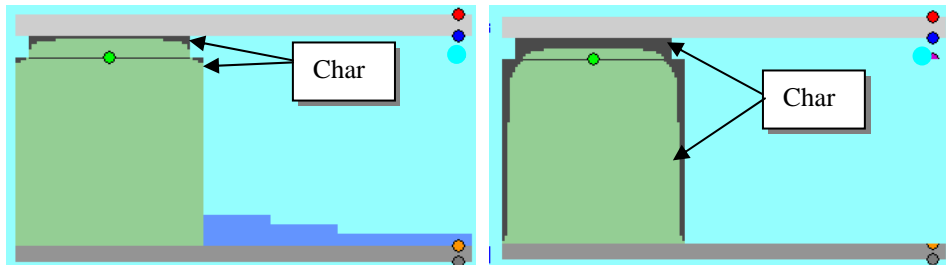


Fig. 8. Melting behavior of foamed insulation and char formation in wood strapping and post at 20 min (left) and 30 min (right).

The model graphically depicts the char formation in wood strapping and also the melting behavior of EPS. Figure 7 shows the melting behavior of EPS at 10 min and 15 min predicted by the model. It was observed that the almost half of EPS already melted at 15 min and char appeared at the corner of the wood strapping. Figure 8 shows the melting behavior of EPS and char formation at 20 min and 30 min predicted by the model. The results show that the thickness of EPS layer was less than 10cm at 20 min and char appeared at the corner of wood post, and at 30 min, char layer spread into strapping and extended along the post surface. It was observed that the whole surface of post was covered with char layer at 30 min. Insulation failure occurred at 42 min 30 sec in the test, while it would be predicted in the model to be 42 min 40 sec, which agrees well with the test results. The ‘fall-off’ of the exterior siding and the gypsum board was not observed.

One more test was conducted for further model validation. As the thickness of EPS in this test was 20 mm (see Fig. 9), there was a big cavity between EPS and gypsum board.

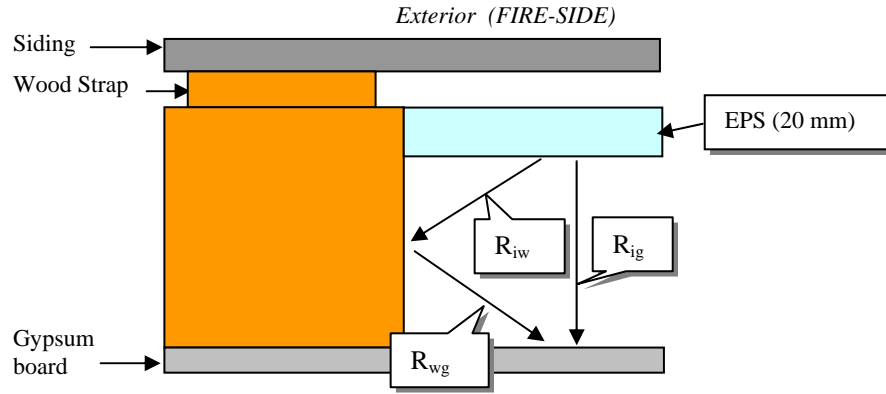


Fig. 9. Structure of the exterior wall with 20 mm thick foamed insulation.

Thereby, new heat transfer equations were considered within this cavity instead of the continuity equations Eqs. 11 and 12. These were the radiative heat transfer from the EPS surface facing this cavity to the side surface of the wood post,  $R_{iw}$  and to the gypsum board surface,  $R_{ig}$ . Thus, the boundary condition at the surface of EPS facing this cavity can be described as,

$$-k_i (\partial T / \partial x) = h_a(T_{is} - T_s) + \epsilon \sigma F_{S12}(T_{is}^4 - T_{gs}^4) + \epsilon \sigma F_{S13}(T_{is}^4 - T_{ws}^4) \quad (14)$$

The boundary condition at the surface of the gypsum board facing the cavity can similarly be written as,

$$-k_g (\partial T / \partial x) = h_a(T_s - T_{gs}) + \epsilon \sigma F_{S12}(T_{is}^4 - T_{gs}^4) + \epsilon \sigma F_{S32}(T_{ws}^4 - T_{gs}^4) \quad (15)$$

And the boundary condition at the surface of the wood post facing the cavity can be described as,

$$-k_i (\partial T / \partial y) = h_a(T_s - T_{is}) + \epsilon \sigma F_{S13}(T_{is}^4 - T_{ws}^4) + \epsilon \sigma F_{S32}(T_{ws}^4 - T_{gs}^4) \quad (16)$$



Where  $F_{S12}$ ,  $F_{S13}$  and  $F_{S32}$  are the view factors for radiative heat exchange [1,2]. Time/temperature curves obtained from the calculated results are shown in Fig. 10, compared to the results from the full-scale test. Solid lines indicate the model prediction and dashed lines test results. A good agreement was observed between them. The time of insulation failure was predicted to be 39 min 45 sec, while it was recorded to be 39 min 30 sec in the full-scale test. Good agreement was also observed between them. The ‘fall-off’ of the exterior siding and the gypsum board was not observed in the tests.

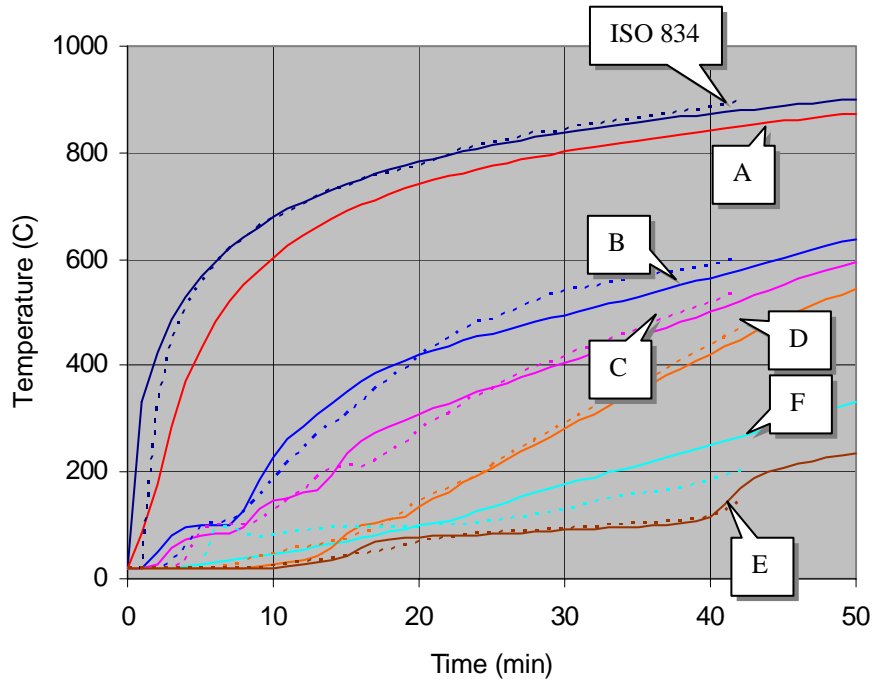


Fig. 10. Model prediction (solid lines) and test results (dashed lines).

### EFFECT OF SIDING THICKNESS AND DENSITY ON FIRE RESISTANCE OF EXTERIOR WALLS

Various types of siding materials are now commercially available with different thickness and different density. Thereby the present study investigated the effect of the thickness and density of the exterior siding on the fire resistance of the exterior walls. In this investigation, it was assumed that the wall was constructed with 105 mm by 105 mm wood post lined by 9.5 mm thick gypsum board as the interior lining and 105 mm thick EPS filled between posts. Density of the exterior siding was assumed to be  $1250 \text{ kg/m}^3$  and the thickness of the exterior siding was changed from 9 mm to 21 mm. Fig. 11 shows the time of insulation failure predicted from the model when the siding thickness changed from 9 mm to 21 mm. The calculated results show that the time of insulation failure would increase from 36 min to 66 min. A significant improvement of fire resistance was observed when the thickness of the exterior siding increases. The time of insulation failure would increase approximately 7 min when the siding thickness increases 2 mm. As a result, the thickness of the exterior siding plays an important role for the fire resistance of this type of exterior walls.

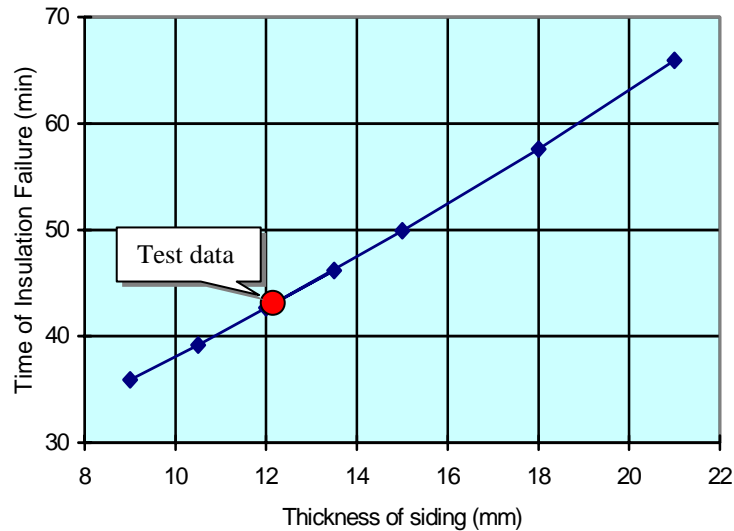


Fig. 11. Time of insulation failure as a function of the thickness of exterior siding ('Test data' shows 42 min 30 sec at 12 mm thick).

Another calculation was conducted to investigate the effect of the siding density on the fire resistance of the exterior walls. In this calculation, the thickness of the exterior siding was assumed to be 12 mm (constant) and the siding density was changed from  $500 \text{ kg/m}^3$  to  $1400 \text{ kg/m}^3$ . Figure 12 shows the time of insulation failure predicted from the model when the siding density increased. It shows that the time of insulation failure would increase only 5 minutes when the density increased from  $500 \text{ kg/m}^3$  to  $1400 \text{ kg/m}^3$ . Thus, the fire resistance of the exterior walls would not be so much improved when the siding density increases.

#### **EFFECT OF GYPSUM BOARD THICKNESS AND DENSITY ON FIRE RESISTANCE OF EXTERNAL WALLS**

There are many different types of gypsum board available in the world. Thereby, the present paper investigated the effect of the thickness and density of gypsum board on the fire resistance of the exterior walls. Calculations were conducted to predict the time of insulation failure when the thickness of gypsum board changed from 9.5 mm to 25 mm with constant density of gypsum board ( $\approx 660 \text{ kg/m}^3$ ). In this calculation, it was assumed that the post size was 105 mm by 105 mm, insulation (EPS) thickness was 105 mm and the thickness of exterior siding was 12 mm.

As shown in Fig. 13, the time of insulation failure predicted from the model would considerably increase with the thickness of gypsum board. Especially the fire resistance would be much improved when the 19 mm and 25 mm thick gypsum boards were used in the wall assemblies.

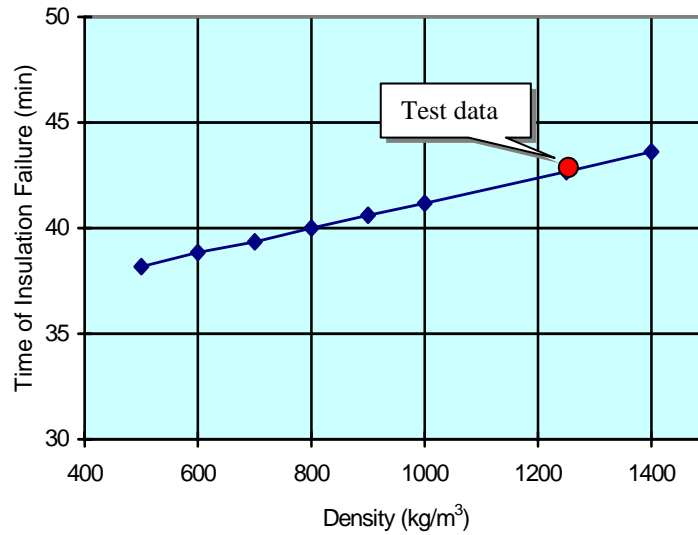


Fig. 12. Time of insulation failure as a function of the density of exterior siding ('Test data' shows 42 min 30 sec at 1250 kg/m<sup>3</sup>).

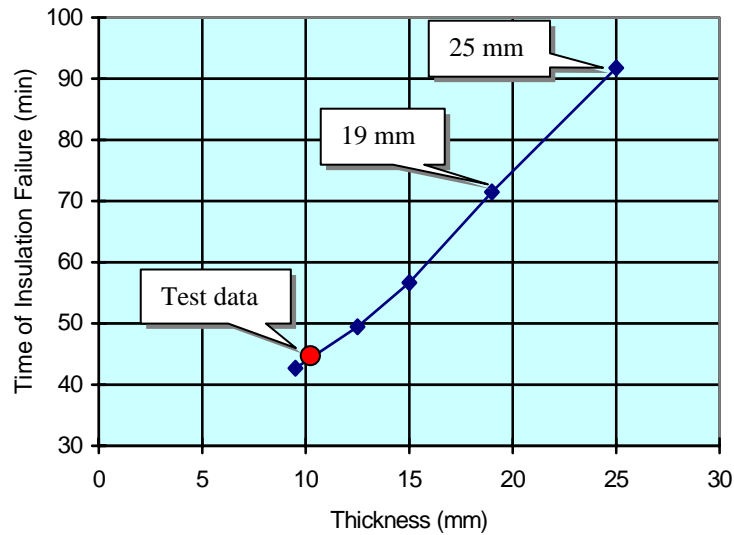


Fig. 13. Time of insulation failure as a function of the thickness of gypsum board ('Test data' shows 42 min 30 sec at 9.5 mm thick).

Final investigation was conducted to examine the effect of density of gypsum board. The density was changed from 500 kg/m<sup>3</sup> to 800 kg/m<sup>3</sup> with constant thickness of gypsum board (=9.5 mm). The results from the computer model indicated that the time of insulation failure would change from 38 min 45 sec to 45 min 55 sec when the density changed from 500 kg/m<sup>3</sup> to 800 kg/m<sup>3</sup>. It seemed that the density of gypsum board would not play an important role for the improvement of the fire resistance. The time of

insulation failure would increase only 7 minutes when the density of gypsum board changed from 500 kg/m<sup>3</sup> to 800 kg/m<sup>3</sup>.

Those results show that the increase of the thickness of siding and also gypsum board would greatly improve the fire resistance of the external walls, while the density of those components, when it increases, would not so much increase the fire resistance.

### CONCLUDING REMARKS

A computer model to predict the fire resistance of the typical 'post and beam' type exterior walls has been developed. Calculated results from the model were compared to the results from the full-scale fire endurance tests, and good agreement was observed. The model also graphically showed the char formation in wood strapping and wood post, and the shrinking and melting behavior of foamed insulation (EPS).

The thickness of exterior siding and gypsum board plays an important role on the fire resistance of the external walls. The model predictions showed that the fire resistance of the exterior walls would greatly be improved when the thickness of exterior siding and gypsum board increased. On the other hand, the density of exterior siding and gypsum board did not play a significant role. The fire resistance of the exterior walls would not be improved so much when the density of those components increased.

### REFERENCES

- [1] Takeda, H., "The Fire Resistance of Wall Assemblies: A New Computer Model, 'HTwall' and Full-Scale Test Data", *Proceedings of the 5th International Conference, Wood and Fire Safety*, Slovakia, 2004, pp. 297-306.
- [2] Takeda, H. and Richardson, L.R., "Fire Resistance of Wood-Framed Exterior Walls: Model and Full-Scale Test," *Proceedings of 8th World Conference on Timber Engineering*, Vol. 2, Finland, 2004, pp. 347-353.
- [3] H. Takeda, "Fire Resistance of Wood-Framed Wall Assemblies: Computer Model and Full-Scale Test", *Proceedings of 8th World Conference on Timber Engineering*, Vol. 2, Finland, 2004, pp. 325-330.
- [4] Takeda, H., "Fire Resistance of Wood-Framed External Walls: The Effect of External Cavity and External Insulation," *Proceedings of 7th International Association on Fire Safety Science*, Worcester, 2002, pp. 1123-1135.
- [5] Takeda, H., "A Model to Predict Fire Resistance of Non-Load Bearing Wood-stud Walls," *Fire and Materials*, 27, pp. 19-39 (2003).
- [6] Takeda, H., "A Computer Model to Predict Fire Resistance of Wood-Framed Exterior Walls," *Proceedings of 7th World Conference on Timber Engineering*, Vol. 2, Malaysia, 2002, pp. 347-353.
- [7] Takeda, H., "A Model to Predict Fire Resistance of Wood-Framed Exterior Walls," *Proceedings of 5th World Conference on the Development of Wood Technology and Forestry*, Ljubljana, 2001, pp. 321-330.
- [8] ISO 834-1: 1999 Fire Resistance Tests-Elements of Building Construction Part1: General Requirements, International Organization for Standardization, Geneva, 1999.